

Full paper

Piezoelectric nanofibrous scaffolds as in vivo energy harvesters for modifying fibroblast alignment and proliferation in wound healing



Aochen Wang^{a,b,1}, Zhuo Liu^{a,c,d,1}, Ming Hu^{b,*}, Chenchen Wang^a, Xiaodi Zhang^a, Bojing Shi^a, Yubo Fan^{c,d}, Yonggang Cui^e, Zhou Li^{a,f,**}, Kailiang Ren^{a,f,**}

^a Beijing Institute of Nanoenergy and Nanosystems, Chinese Academy of Sciences, Beijing 100083, China

^b Microelectronics and Solid State Electronics, School of Microelectronics, Tianjin University, Tianjin 300192, China

^c Key Laboratory for Biomechanics and Mechanobiology of Ministry of Education, School of Biological Science and Medical Engineering, Beihang University, Beijing 100083, China

^d Beijing Advanced Innovation Center for Biomedical Engineering, Beihang University, Beijing 102402, China

^e Department of Nuclear Medicine, Peking University First Hospital, Beijing 100034, China

^f CAS Center for Excellence in Nanoscience, National Center for Nanoscience and Technology (NCNST), Beijing 100190, China

ARTICLE INFO

Keywords:

Electrospinning

P(VDF-TrFE) nanofibrous scaffolds

In vivo energy harvester

Wound healing

ABSTRACT

Since the last decade, piezoelectric polymer nanofibers have been of great interest in the stimulation of cell growth and proliferation for tissue engineering and wound healing applications. To date, there is no clear understanding of how the piezoelectric properties of piezoelectric materials can be affected by electrospinning parameters and how the piezoelectricity from the electrospun polymer nanofibers produced under optimized electrospinning conditions in vivo would affect cell growth, proliferation and elongation. In this paper, it is shown for the first time how electrospinning parameters, such as solution concentration and collecting distance (from the needle to the rotating mandrel), can affect the piezoelectricity of the poly(vinylidene fluoride-trifluoroethylene) (P(VDF-TrFE)) nanofibers. Here, the optimized electrospinning conditions for P(VDF-TrFE) nanofibers were achieved and these nanofiber scaffolds (NFSs) were used for implanted energy harvester in SD rats, cell proliferation and cell alignment growth applications. During the process of slightly pulling implanted site of SD rats, the implanted P(VDF-TrFE) NFSs generated a maximum voltage and current of 6 mV and ~6 nA, respectively. With great cytocompatibility and relatively large piezoelectric effect, fibroblast cells grew and aligned perfectly along the electrospinning direction of P(VDF-TrFE) nanofiber direction and cell proliferation rate was enhanced by 1.6 fold. Thus, electrospun P(VDF-TrFE) NFSs show great promise in tissue engineering and wound healing applications.

1. Introduction

In 1940, Burr et al. found for the first time that a surface electro-potential exists over the healing section in patients after surgery [1]. In late 1950s, Fukada et al. first reported piezoelectricity in bones [2]. In the 1960s, Becker discovered that a direct current (DC) existed between regenerating and nonregenerating tissue in amphibians [3]. In the late 1960's, Assimacopoulos found that a skin defect treated by DC current in rabbit ears showed 25% acceleration of wound healing as compared with untreated defective areas [4]. Since then, the potential for wound healing and the utilization of electrical charges to stimulate cell proliferation have been the subject of intensive research [5,6]. Recently,

studies have demonstrated that piezoelectric and electret materials can be used to produce enough surface charge to stimulate the proliferation or differentiation of a variety of cells [7–10]. In this paper, it is shown for the first time how electrospinning parameters, such as solution concentrations and collecting distances from the needle to the rotating mandrel, affect the piezoelectricity of the poly(vinylidene fluoride-trifluoroethylene) (P(VDF-TrFE)) nanofibers. After the P(VDF-TrFE) nanofibrous scaffolds (NFSs) were fabricated under optimized electrospinning conditions, the cell proliferation rate was enhanced 1.6 fold when the poled P(VDF-TrFE) NFSs were stimulated by mechanical vibration inside a Flexcell culture plate.

From the literature, poly(vinylidene fluoride) (PVDF) and its

* Corresponding author.

** Corresponding authors at: Beijing Institute of Nanoenergy and Nanosystems, Chinese Academy of Sciences, Beijing 100083, China.

E-mail addresses: zli@binn.cas.cn (Z. Li), renkailiang@binn.cas.cn (K. Ren).

¹ These authors contributed equally to this work.

copolymer poly(vinylidene fluoride-trifluoroethylene) (P(VDF-TrFE)) exhibit the largest piezoelectric response compared with other piezoelectric polymers such as nylon, poly(lactic acid) (PLA), or poly-hydroxybutyrate (PHB) [11]. Most PVDF based polymers possess α , β , and γ phases, depending on the polymer processing conditions [10]. Normally, stretched PVDF polymer films exhibit a much higher crystalline β phase than unstretched films [12]. Unlike PVDF, P(VDF-TrFE) can possess all-trans configuration without mechanical stretching [13]. Recently, due to its relatively large piezoelectricity, chemical stability, ease of processing, and biocompatibility, P(VDF-TrFE) has been used in bone regeneration and neural tissue engineering applications [14–16].

Guo et al. have investigated the electrospun PVDF/polyurethane (PU) membrane as a scaffold for wound healing applications [17]. However, an electrospinning process normally possess a lower stretching ratio than a normal film fabrication process. This could be the reason that the PVDF nanofibers possess low piezoelectricity in that experiment. Recently, many researchers have also investigated various PVDF nanocomposites to stimulate various cells or promote bone regeneration [18,19]. However, the piezoelectric nanocomposite normally has much lower biocompatibility with biological systems, which makes it difficult to use directly on human beings. Previously, we have shown that electrospinning has been used as a unique method to produce piezoelectricity in various piezoelectric polymers [20–22]. Additionally, due to their high surface-to-volume ratio and substantial porosity, electrospun nanofibers offer great advantages for applications in cell adhesion, migration and growth.

In our previous publications, we have shown that the PVDF nanofibers produced by conventional electrospinning methods showed no piezoelectricity [20]. To produce the piezoelectricity in electrospun piezoelectric polymers, P(VDF-TrFE) was chosen in this investigation to study how various electrospinning parameters, such as solution concentration and collecting distance from the syringe needle to the rotating mandrel, affect the morphology of the P(VDF-TrFE) nanofibrous scaffolds. After the optimized electrospinning condition was obtained, the fabricated P(VDF-TrFE) nanofibers were utilized for cell adhesion, migration and proliferation applications. From the testing results of 3-(4, 5-dimethylthiazol-2yl)-2, 5-diphenyl-2H-tetrazolium bromide (MTT), it was found that fibroblast cells spread out and align perfectly along the electrospinning direction of P(VDF-TrFE) NFS. After the cell proliferation assay, the cell proliferation rate can increase by 60% after stimulation by the poled P(VDF-TrFE) NFSs. This research result proves that electrospun P(VDF-TrFE) NFSs have great promise in tissue engineering and regeneration applications.

2. Experimental section

2.1. Fabrication of P(VDF-TrFE) nanofibrous scaffolds

As explained in previous papers, the P(VDF-TrFE) nanofibers were fabricated using a lab-designed conventional electrospinning setup [20]. To prepare the polymer solution, P(VDF-TrFE) (75/25) (Piezotech Inc., France) was dissolved in a mixture solvent of N-Dimethylformamide (DMF) and acetone (6:4) with varied solution concentrations of 15%, 18% and 20% (w/v). After the polymer solution was injected into a syringe, the electrospinning process was conducted with a constant flow rate of 1 ml/h using a syringe pump (KDS101, KD Scientific, USA). A DC voltage of 15 kV was applied between the syringe needle and the rotating mandrel (2000 rpm speed), where the mandrel was wrapped with 2 cm wide aluminum foil to collect the aligned P(VDF-TrFE) fibers. The collecting distances were set at varied spaces of 5 cm, 10 cm and 15 cm. Afterward, the fabricated P(VDF-TrFE) NFSs were dried at 65 °C in an oven for 10 h to completely evaporate the residual solvent. Next, these nanofibers were annealed in an oven at 135 °C for 4 h to increase the crystallinity. To obtain a smooth surface, the nanofiber samples were pressed with a hot press machine (TY605-8T, Yuyao Tianyu Machinery Equipment Co. Ltd, China) at room temperature. Further, the

pressed P(VDF-TrFE) NFS was sputtered with Au electrodes on the top and bottom sides of the sample and then poled in a silicon oil bath under an electric field of 100 MV/m at 115 °C for 30 min to obtain high piezoelectricity. Prior to cell culturing, P(VDF-TrFE) NFSs were cut into a dimension of 2 cm × 2 cm pieces and sterilized in 75% ethanol for 30 min and then exposed to ultraviolet (UV) light for one hour.

The microscopic images of electrospun NFSs were characterized by a SU8020 scanning electron microscope (Hitachi Ltd., Japan). The average fiber diameter was evaluated using image-J software. The differential scanning calorimetry (DSC) measurement of P(VDF-TrFE) NFSs was analyzed at 10 °C/min in a nitrogen environment by a TGA/DSC1 (Mettler-Toledo LLC., Columbus, OH, USA) from 40 °C to 180 °C. X-ray diffraction (XRD) patterns were performed by a PANalytical X'pert³ diffractometer (PANalytical Ltd., Netherland) using a Cu K α source with a step size of 0.013° from a 10° to 50° range. FTIR spectra were performed on Vertex80V (Bruker Corp., USA) and Fourier transformation infrared spectrometer analysis was performed in the range of 400–1600 cm⁻¹ with a resolution of 4 cm⁻¹.

Before the piezoelectric properties measurement, the electrospun PVDF-TrFE nanofibers were pressed under a high pressure using a hot press machine at room temperature. The pressed electrospun nanofiber film was sputter coated with Au electrodes on both sides of the surfaces. Next, the sample was poled inside a silicone oil at 100 °C under 2 kV for 30 mins in a lab designed poling setup. Afterwards, the sample was kept under same voltage and cooled down to room temperature slowly.

As explained in previous publications, the piezoelectric coefficient d_{31} was measured using a lab-designed piezoelectric coefficient measurement setup, which consists of a supporting frame, a load cell, a shaker and a lock-in amplifier [23,24]. After being poled at 100 MV/m at 100 °C for 30 min, the hot-pressed P(VDF-TrFE) nanofiber scaffold was cut into a rectangular strip (20 mm × 10 mm). During the piezoelectric coefficient measurement, the force applied to the P(VDF-TrFE) nanofibers was measured by a load cell (ELPF-50N-C3006, Measurement Specialties Inc, VA, USA). The generated electrical signal was measured by a lock-in amplifier. (SR830, Stanford Research Systems Inc., CA, USA).

2.2. In vivo animal assay

Polarized P(VDF-TrFE) NFSs were encapsulated in polydimethylsiloxane (PDMS) using a solution casting method and then were cut to a dimension of 20 mm (L) × 20 mm (W). To confirm the piezoelectric response of polarized P(VDF-TrFE) NFS in vivo, these NFS scaffolds were implanted into the subcutaneous thigh region of highly active Sprague Dawley (SD) rats (male, 200–250 g, the Academy of Military Medical Sciences, China). To simulate the movement of SD rate, a linear motor system (LinMot USA, Inc., Elkhorn, WI, USA) was used to gently pull a leg of the SD rat. The pulling force was around 0.5 N with 1 Hz frequency. The procedures strictly followed the “Beijing Administrative Rules for Laboratory Animals” and the national standard “Laboratory Animal Requirements for Environment and Housing Facilities (GB 14925-2001).” The generated electrical outputs were recorded by an oscilloscope (DPO3034, Tektronix, USA). The procedure for anesthetizing the rat started with the intake of isoflurane gas (1–3% in pure medical grade oxygen), followed by the injection of 1% sodium pentobarbital (intraperitoneal, 40 mg kg⁻¹) for anesthesia induction and maintenance, respectively.

2.3. Primary culture of L929 cells

2.3.1. Dynamic culture of L929 fibroblast cells

In this test, specialized flexible-bottomed culture plates (BF-3001U, Flexcell International Corporation, USA) were used to culture the fibroblast cells. As shown in Fig. 1(a), the pressed P(VDF-TrFE) NFSs were glued to the bottom of the bioflex culture plate. To generate a mechanical vibration, a lab-designed speaker was attached tightly on

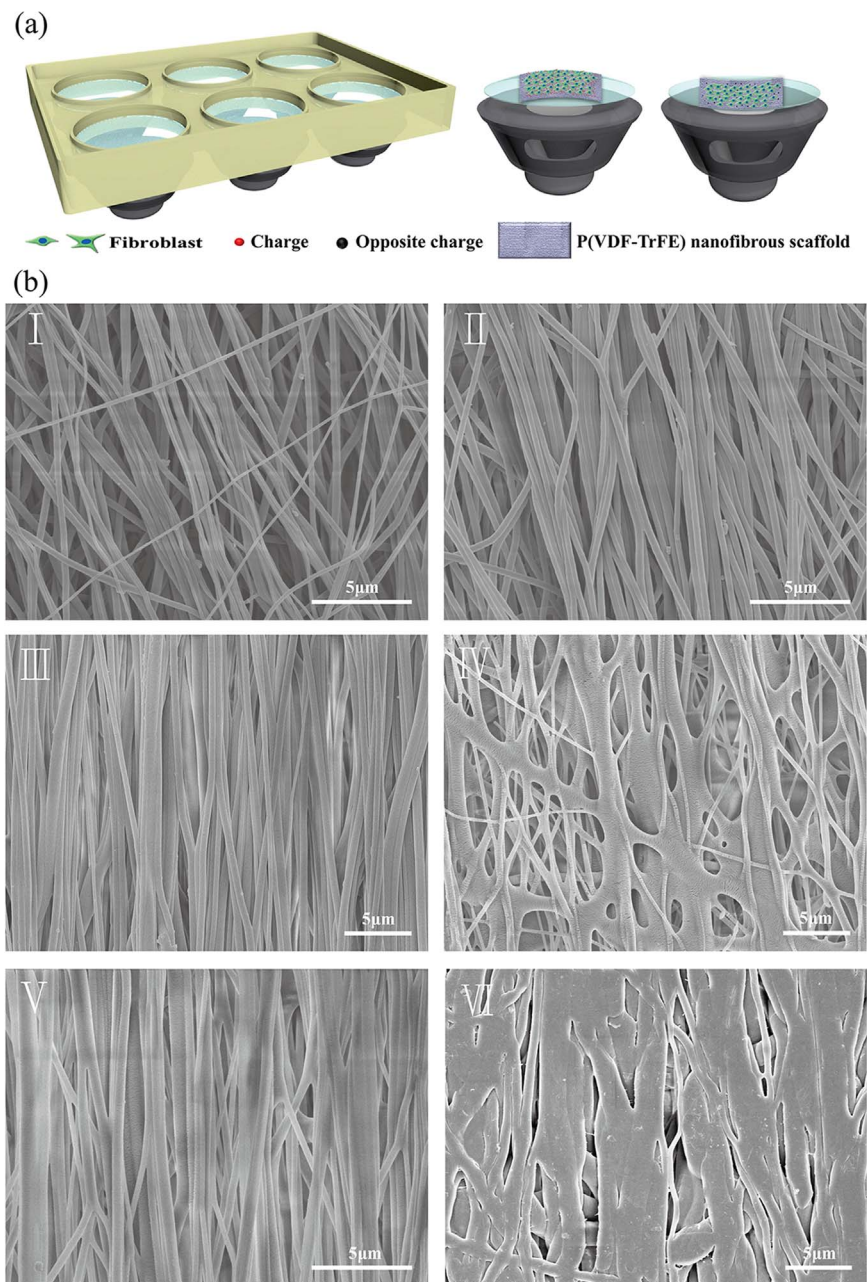


Fig. 1. (a) Schematic drawing of experimental setup where the speaker is utilized to excite the piezoelectricity of electrospun P (VDF-TrFE) scaffolds on the flexible bottom culture plate. (b) Scanning electron microscope (SEM) images of electrospun P (VDF-TrFE) nanofibers fabricated under varying solution concentrations and various collecting distances after annealing: (I) 15%, 10 cm (II) 18%, 10 cm (III) 20%, 10 cm (IV) 20%, 5 cm (V) 20%, 15 cm (VI) 20%, 10 cm, pressed. The insets are the higher magnification of the surface morphologies of the PVDF nanofibers.

the bottom of the flexi-bottom cell culture plates using a silicone rubber holder. A signal was generated from a function generator (DS345, Stanford Research Systems, Inc., CA, USA) and then amplified by a power amplifier (Xli202, Crown Audio Inc., Elkhart, USA) to control the frequency and the vibration of the culture plates.

After being cultured for 72 h, L929 fibroblast cells were seeded in the bioflex culture plate with a density of 5×10^4 cells/ml. The poled P (VDF-TrFE) NFSs were the experimental group, while the unpoled P (VDF-TrFE) NFSs and tissue culture polystyrenes (TCPS) served as the control group. Next, the proliferation of the cultured L929 fibroblast cells was analyzed using a 3-(4, 5-dimethylthiazol-2-yl)-2, 5-diphenyl-2H-tetrazolium bromide (MTT) assay. The cells were first incubated with the MTT solution (100 μ L) in an incubator at 37 $^{\circ}$ C for 4 h. Then, the culture medium was removed, and the insoluble formazan was dissolved in 500 μ L dimethyl sulfoxide (DMSO) solvent in each well. The absorbance of the solution was measured using a microplate reader (Multiskan MK3, Thermo Fisher Scientific Inc., USA) at a wavelength of 490 nm. The analytical assays were conducted at day 1, day 3, and day

5 under both static and dynamic vibration conditions. In dynamic vibration condition, the speaker was driven by a 3 Hz sinusoidal signal for a period of 1 h excitation at an interval of 1 h. This process was repeated five times per day for every cell culture plate. In this investigation, every experiment was repeated three times to obtain consistent results.

The cytoskeleton and nucleus were stained with Phalloidin and 4', 6-diamidino-2-phenylindole (DAPI), respectively. Specifically, the L929 fibroblast cells were fixed by an immunohistochemical (IHC) fixation method (Beyotime Biotechnology, China) for 30 min, then washed three times with warm Phosphate Buffered Saline (PBS), then blocked with 0.1% Bovine Serum Albumin (BSA) solution for one hour at 37 $^{\circ}$ C. Afterward, the cells were incubated with diluted DAPI (1:400) (Sigma-Aldrich Corp., MO, USA) and stained by Alexa Fluor 568 phalloidin (1:200) (Thermo Fisher Scientific Inc., USA) for two hours at 37 $^{\circ}$ C.

After 48 h of incubation, the rinsed cells were fixed with 2.5% glutaraldehyde for two hours. Subsequently, a series of alcohol solutions (30%, 50%, 70%, 80%, 90%, 95%, 98%, and 100%) was applied

to dehydrate the cells. The cell SEM images were taken by Hitachi SU8020 SEM (Hitachi Ltd., Japan).

3. Results and discussion

3.1. Surface morphology

The microscopy images of electrospun P(VDF-TrFE) NFSs are shown in Fig. 1(b). As shown in the Supporting information in Fig. S1, once the solution concentrations are increased from 15% to 18% and then to 20% (w/v), the diameters of the nanofibers increase from 350 nm to 360 nm and then to 510 nm. The nanofibers fabricated using the 20% concentration exhibit more homogenous characteristics and less branching than under lower concentrations. As Fig. 1(b) shows, the P(VDF-TrFE) NFSs fabricated under the 5 cm collecting distance (from the rotating mandrel to the needle) show a large degree of fiber surface adhesion and branches. This phenomenon can be explained by the observation that the short collecting distance does not completely evaporate the solvent inside the fiber and therefore cause surface adhesion. When the collecting distance is tuned to 10 cm, the P(VDF-TrFE) NFSs are perfectly aligned along the electrospinning direction with great uniformity. From the microscopy images shown in Fig. 1, it is obvious that the poled P(VDF-TrFE) scaffold keeps its porous structure after annealing. The porous structure could create a transportation path for nutrients and implanted cells.

This experiment demonstrated that the electrospinning parameters, such as the solution concentration and the collecting distance, play a critical role on the morphology of P(VDF-TrFE) NFSs. It was found that the optimized fiber morphology can be obtained once the solution concentration of 20% (w/v) and collecting distance of 10 cm were chosen during the electrospinning process. In the following, the crystallinity and the piezoelectricity of the P(VDF-TrFE) NFSs also were tested under these electrospinning conditions to achieve the maximum piezoelectricity in P(VDF-TrFE) NFSs.

3.2. Crystalline characterization

The XRD diffraction patterns of P(VDF-TrFE) NFSs fabricated at various electrospinning conditions are shown in Fig. 2(a). From the data, there is a distinct diffraction peak around 20° for all NFSs, which corresponds to the diffraction of the plane (200)/(100) of the β phase crystal [25,26]. Among the nanofibers fabricated at a distance of 5 cm, 10 cm and 15 cm, the P(VDF-TrFE) NFSs fabricated at a collecting distance of 10 cm show the highest diffraction peak (Fig. 2(a)).

To elucidate the effect of the collecting distance on the crystallinity of the electrospun P(VDF-TrFE) nanofibers, the crystal structure was

characterized by Fourier transform infrared (FTIR) measurement. As shown in Fig. 2(b), the characteristic absorption bands at 840 , 1430 cm^{-1} are associated with a β phase structure, whereas the absorption peaks at 615 , 763 , 854 , 974 cm^{-1} are associated with an α phase structure [25,26]. From the data shown in Fig. 2(b), the nanofibers fabricated at a collecting distance of 10 cm show a much enhanced absorption peak at 1430 cm^{-1} as compared with the ones fabricated at collecting distances of 5 cm and 15 cm. This means that the nanofibers fabricated with a 10 cm collecting distance possess a much higher β phase than those collected under other electrospinning conditions. These data is consistent with the XRD results shown in the last paragraph. There is no observed α phase crystal in the FTIR data, suggesting that the electrospun P(VDF-TrFE) is mostly in the β phase. Theoretically, a relative longer collecting distance will improve the solvent evaporation, and the shear force from the electrostatic force applied on the P(VDF-TrFE) nanofiber will stretch the nanofibers and make them exhibit more β phase conformation.

The XRD diffraction patterns and FTIR spectra indicate that the optimized electrospinning conditions for P(VDF-TrFE) nanofibers are with the collecting distance of 10 cm and solution concentration of 20%. The NFSs fabricated under these conditions possess more β phase than those fabricated under other electrospinning conditions.

The effect of thermal treatment on the Curie transition temperature (T_c) of NFSs was further analyzed by DSC. DSC thermograms of annealed and unannealed P(VDF-TrFE) nanofibers are shown in Supporting information in Fig. S2. The Curie transition temperature (T_c) of annealed P(VDF-TrFE) nanofibers is much higher than the T_c without annealing. These results demonstrate that the annealing process enhances the crystallinity of electrospun P(VDF-TrFE) nanofibers. Additionally, from the DSC thermogram, the annealed nanofibers show much sharper endothermic peaks than the as-spun P(VDF-TrFE) nanofibers. This could result from the enhanced crystallinity in the P(VDF-TrFE) NFS after annealing. Further, the melting temperature (T_m) of the annealed P(VDF-TrFE) nanofibers also was increased. These data are related to the crystallinity as well as the increased amount of all-trans conformation (β phase) of NFSs. It can be concluded that thermal treatment will induce all-trans conformation and thus increase the crystallinity of the nanofibers.

3.3. Piezoelectric coefficient measurement

The piezoelectric coefficient d_{31} of the electrospun P(VDF-TrFE) fabricated at various collecting distances was measured using a lab-designed piezoelectric measurement setup as described in our previous publications [23,24]. The setup mainly consists of a load cell, a loud-speaker and a lock-in amplifier. All the compressed nanofibers were

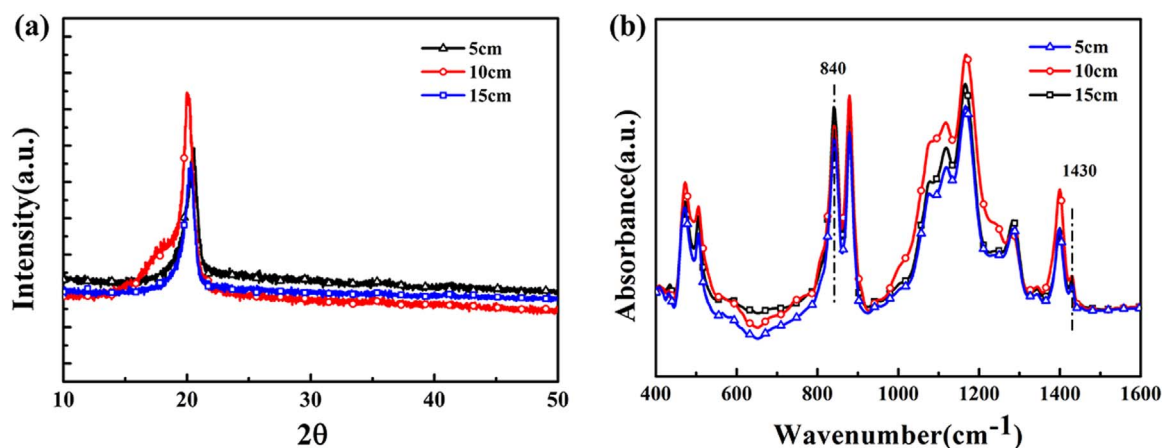


Fig. 2. Crystallization of electrospun P(VDF-TrFE) with 20% solution concentration and varying collecting distances (a) X-ray diffraction (XRD) patterns (b) Fourier transform infrared spectra.

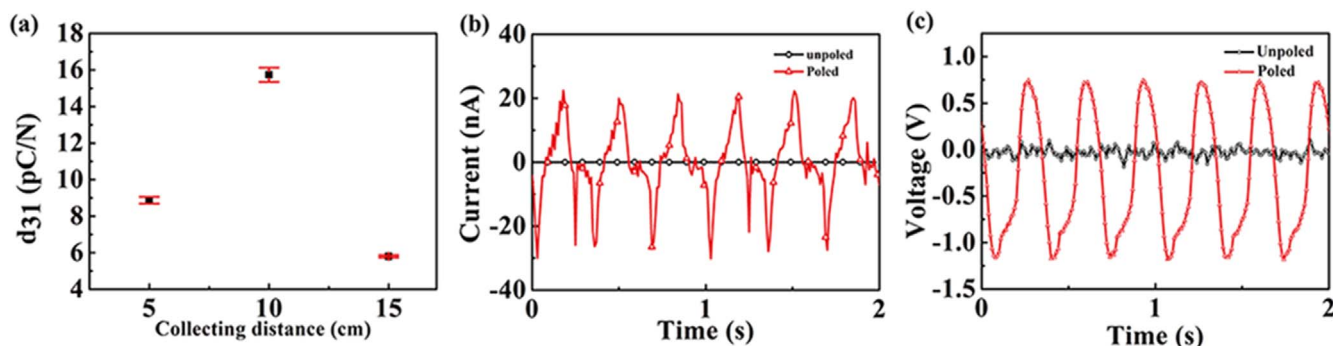


Fig. 3. Characterization of electrospun P(VDF-TrFE) nanofiber scaffolds (a) Piezoelectric coefficient d_{31} of the scaffolds under varying collection distances (from the needle to the rotating mandrel) (b) Current output (c) Voltage output of the scaffolds with different thermal treatment.

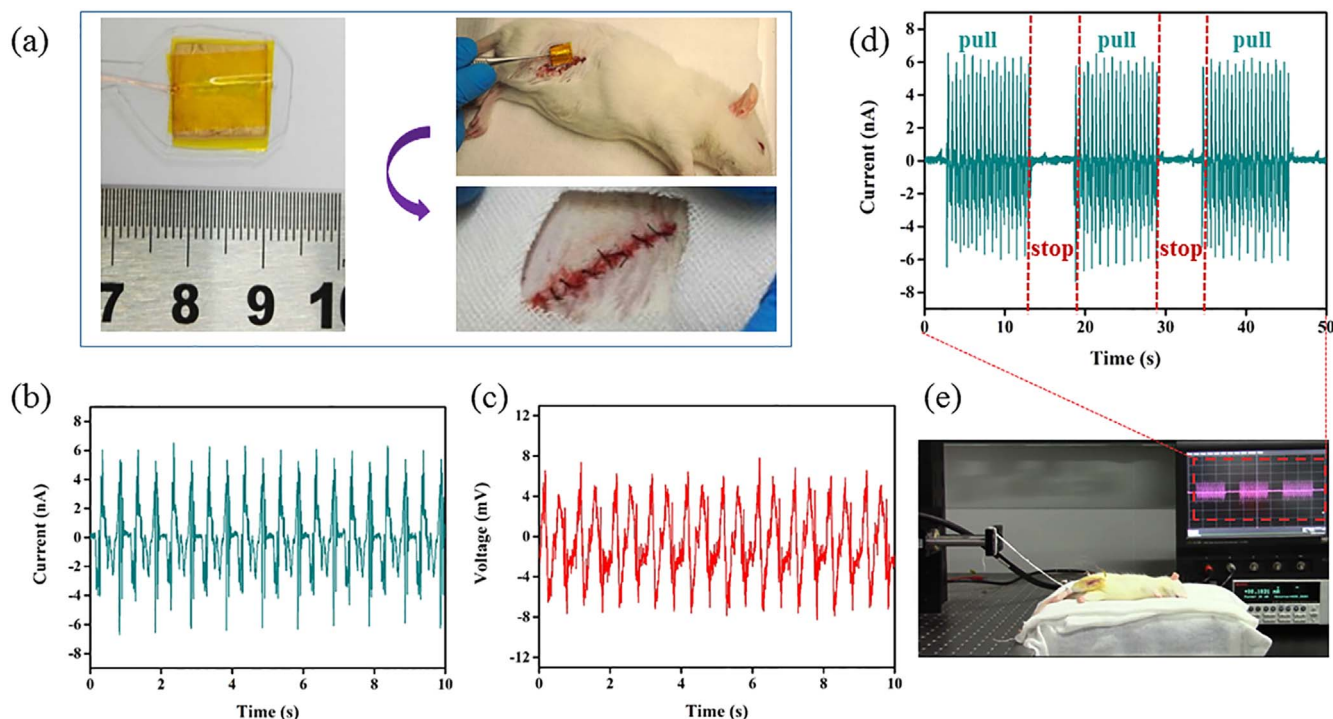


Fig. 4. *In vivo* voltage and current output of the electrospun P(VDF-TrFE) nanofiber scaffolds under pulling conditions. (a) Image of electrospun P(VDF-TrFE) nanofiber scaffolds before implantation (left) and the demonstration process of implanting in the subcutaneous thigh region of a Sprague Dawley (SD) rat (upper right) and the implanting site after suturing (lower right). (b) Current output and (c) Voltage output of the implanted P(VDF-TrFE) nanofiber scaffolds (d) Current output of the implanted scaffolds with intermittent pulling (pulling-releasing) (e) Image of the experimental setup.

poled at 100 °C in an electric field of 100 V/ μ m for 30 min. The measurement data is shown in Fig. 3(a). From the data, it is revealed that the electrospun P(VDF-TrFE) NFSs with collecting distance of 10 cm show the highest piezoelectric coefficient d_{31} of 15.73 pC/N.

From the data shown in the SEM images and the XRD results, the electrospun PVDF-TrFE nanofibers fabricated at the collecting distance of 10 cm and with the solution concentration of 20% show perfect alignment. On the other hand, the collecting distance of 15 cm may reduce the electrostatic force and cause random distribution of the nanofibers. This is the reason that the electrospun PVDF-TrFE nanofibers fabricated at the collection distance of 15 cm possess a lower piezoelectric coefficient. Compared with the collecting distance of 5 cm, a longer collecting distance (10 cm) can induce a larger stretching ratio during the electrospinning process and eventually cause a relative larger piezoelectric coefficient. Compared with other solution concentrations, the 20% polymer solution produced uniform nanofibers without beads, which improved fiber quality and eventually piezoelectricity. Theoretically, a higher solution concentration normally cause coagulation in electrospinning process and a lower solution

concentration may induce discontinuity in the fiber. Therefore the electrospinning condition with a solution concentration 20% and the 10 cm distance is the optimized electrospinning conditions to produce the PVDF-TrFE nanofibers with enhanced piezoelectricity. The measurement result of piezoelectric coefficient is consistent with the XRD diffraction and FTIR results.

Further, the polarization as a function of the electric field (P-E) loop of the electrospun P(VDF-TrFE) NFS was measured by a Precision Premier II Ferroelectric Tester (Radiant Technologies Inc., New Mexico, USA). The P(VDF-TrFE) nanofibers were fabricated under the optimized electrospinning conditions (20% solution concentration, 10 cm collecting distance). As shown in Supporting information in Fig. S3, the annealed and unannealed P(VDF-TrFE) NFSs were tested. It was found that the remnant polarization (P_r) of P(VDF-TrFE) NFS can increase from 45 mC/m² to 65 mC/m² after annealing. Similarly, the saturated polarization (P_s) under the same electric field can reach 81 mC/m² under a 179 MV/m electrical field. These results suggest that the electrospun P(VDF-TrFE) nanofibers performs mostly in the β crystal phase after annealing treatment.

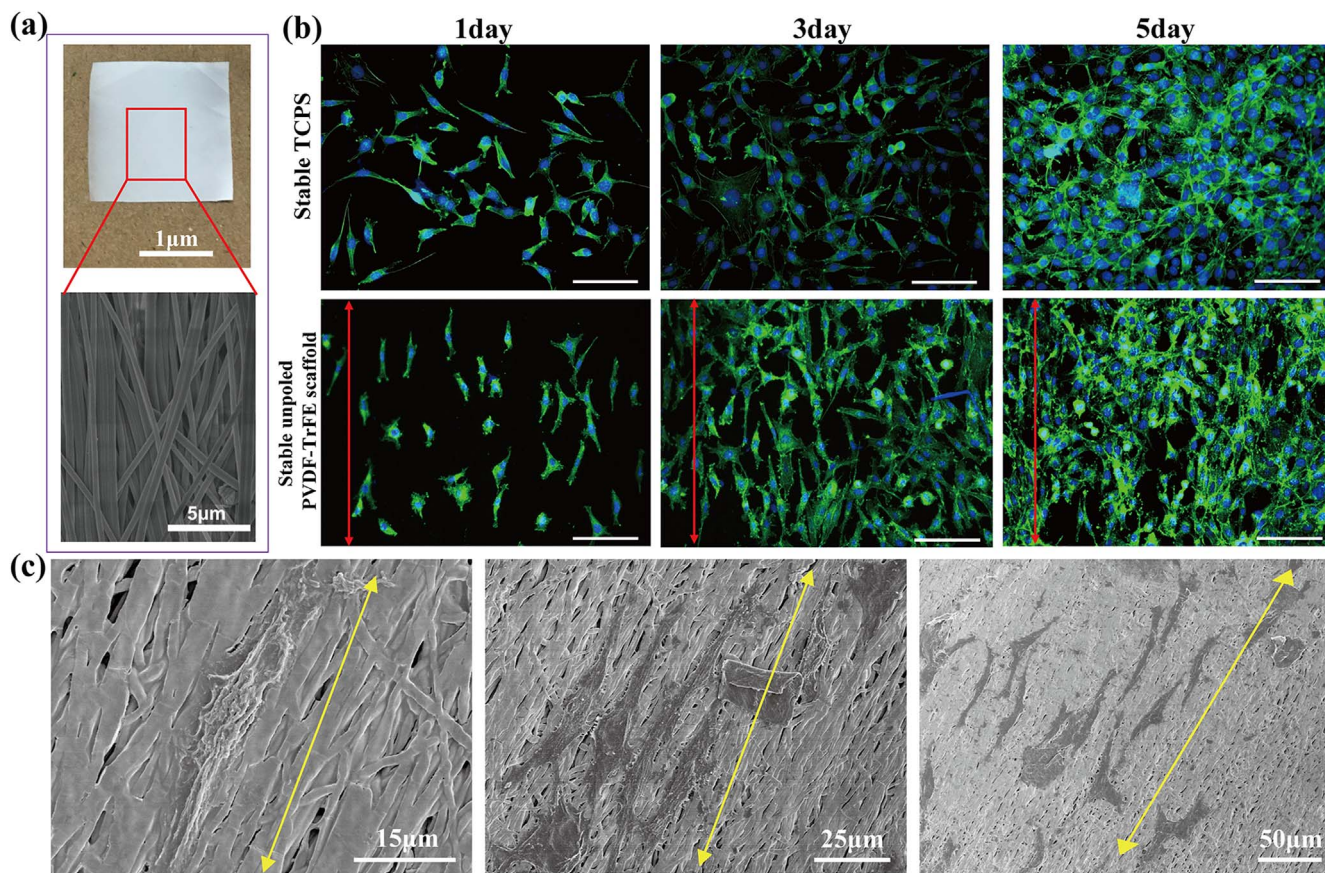


Fig. 5. *In vitro* cytocompatibility of L929 fibroblast cells on the stable electrospun P(VDF-TrFE) nanofiber scaffolds. (a) Photograph (above) and Scanning Electron Microscope (SEM) (below) of P(VDF-TrFE) nanofiber scaffolds (b) Fluorescence microscopy images of L929 fibroblast cells on tissue culture polystyrenes (TCPS) (above) and P(VDF-TrFE) nanofiber scaffolds (below) after a three-day culture. The actin network was stained by Alexa Fluor 488-labeled phalloidin (green) and the nucleus was stained by 4',6-diamidino-2-phenylindole (DAPI) (blue). (c) Elongation images of L929 fibroblast cells on P(VDF-TrFE) nanofiber scaffolds with various magnifications.

3.4. Electric output

During this experiment, the electrospun P(VDF-TrFE) nanofibers were pressed together using a hot press machine, as explained above. After the sputter coated samples were poled at 100 MV/m at 100 °C for half an hours, the output current and voltage of the sample were measured using the same setup as the one used for the piezoelectric coefficient d_{31} measurement. From the data shown in Fig. 3(b) and (c), it was found that the output voltage could reach more than 1.5 V (peak-peak) and the output current was about 52.5 nA (peak-peak). For annealed and unpoled P(VDF-TrFE) fiber scaffolds, the samples showed almost no output signal. Even though the P(VDF-TrFE) nanofibers exhibit mostly β phase conformation after electrospinning, the material still needs extra-poling steps to obtain piezoelectricity because the dipoles are arranged in random orientation.

3.5. *In vivo* piezoelectric response

In vivo energy generation by the natural body activity and physiological environment has been reported recently [27–29]. In order to effectively evaluate the electrical output of the P(VDF-TrFE) NFSs in wound area, a polarized P(VDF-TrFE) scaffold was implanted under the skin of the leg of SD rats. The action of pulling was used to mimic the daily activity of rats. In the testing process, a linear motor was used to pull up the leg of the rat through a wire (Fig. 4c). As shown in Fig. 4(b), the voltage output of a poled P(VDF-TrFE) NFS can be clearly identified by pulling on a rat's leg and then pausing. In the process of pulling up the rat's leg, the peak output voltage and output current of a polarized P(VDF-TrFE) NFS reached ~ 6 mV and around ~ 6 nA (Fig. 4e),

respectively. The results indicate that the P(VDF-TrFE) NFS implanted in wound area can also generate adequate piezoelectric output through the rat's daily activity to stimulate cell activity, and demonstrated the stability and property for *in vivo* applications.

3.6. *In vitro* cytocompatibility of P(VDF-TrFE) NFSs

For tissue engineering and wound healing applications, the cytocompatibility of biological scaffolding material is one of the most critical requirements for the use of such material in cell growth, alignment and proliferation applications [30]. In this investigation, the viability of L929 fibroblast cells in P(VDF-TrFE) NFSs and tissue culture polystyrenes (TCPS) was evaluated over a three-day period by MTT assay. As shown in Supporting information of Fig. S2, the results show no significant differences in the quantity of cells between the stable P(VDF-TrFE) NFSs group and the stable TCPS group. The result is consistent with previous literature in which the P(VDF-TrFE) biomaterial scaffolds have good biocompatibility for various cells such as cardiovascular cells, nerve cells and human skin fibroblasts [14–16]. As seen in the confocal fluorescence micrographs shown in Fig. 5(c), the fibroblast L929 cells align perfectly along the electrospinning direction of P(VDF-TrFE) NFSs. On the other hand, the cells cultured on TCPS exhibit relatively random orientation. This demonstrates that P(VDF-TrFE) NFSs fabricated under the optimized process conditions show excellent cytocompatibility. Moreover, as shown in the SEM graphs in Fig. 5(c), the L929 cells elongate perfectly along the nanofiber direction. This result indicates that aligned P(VDF-TrFE) NFSs can provide a suitable three-dimensional surface for L929 cell adhesion and growth.

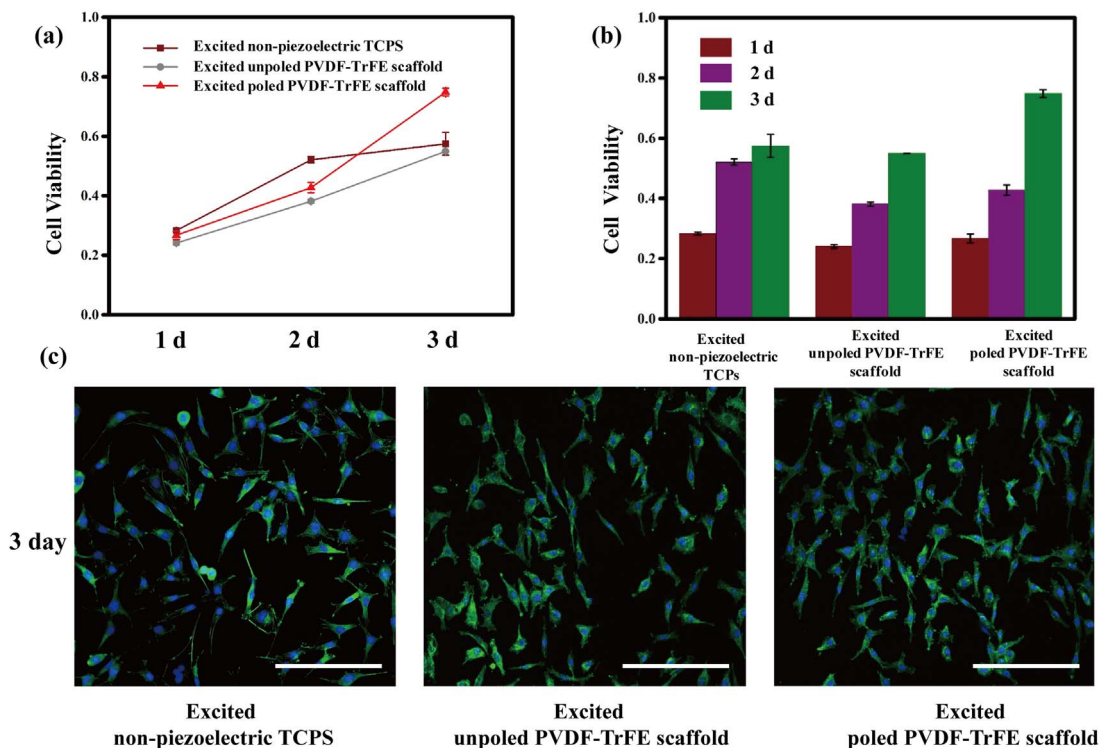


Fig. 6. *In vitro* piezoelectric effect of electrospun P(VDF-TrFE) nanofiber scaffolds on L929 fibroblast cell proliferation under dynamic stimulus. (a) Plot and (b) Bar chart of the proliferation of L929 fibroblast cells on excited tissue culture polystyrenes (TCPS), excited unpoled P(VDF-TrFE) scaffolds and excited poled P(VDF-TrFE) scaffolds after 1, 2, and 3 days culture. (c) Fluorescence microscopy images of L929 fibroblast cells on electrospun P(VDF-TrFE) nanofiber scaffolds and tissue culture polystyrenes (TCPS) after a three-day culture (scale bar 200 μm).

3.7. *In vitro* cells proliferation

Before the cell proliferation test, both sides of the film surface were cleaned with Acetone to completely remove the silicone oil and the Au electrode. Normally a piezoelectric material needs a poling process to align all the dipoles along one direction in the material. In this investigation, the pressed nanofibers were put inside a PBS solution in the Flexcell culture plates. When the nanofibers were vibrated by the speaker underneath the culture plate, the surface charges were generated on the top and bottom electrodes, which can increase the cell growth and proliferation as result.

In the experiment, the poled and unpoled P(VDF-TrFE) nanofiber scaffolds were used to analyze the effect of dynamic piezoelectric stimulus on L929 fibroblast cells. The proliferation assays were divided into three groups and cultured for three days as standard protocol for cell proliferation measurement: Group I was the poled P(VDF-TrFE) nanofiber scaffold as active material; Group II was the unpoled P(VDF-TrFE) nanofiber scaffold (NFS). Group III was TCPS. Group I was the test group, and Groups II and III were the reference groups. The experimental results are shown in Fig. 6. From the data, the quantity of cells shows no apparent differences between the three groups over a one-day culture (Fig. 6a, b). On day 2, it was found that the proliferation of L929 fibroblast cells on TCPS was much higher than the other two groups under dynamic stimulus, while cell proliferation rates for all groups were almost equal. As compared to the cells on day 2, the proliferation rate of the cells in Groups III, II and I after day 3 were approximately 1.103-, 1.43-, 1.75-fold, respectively. This means that cell proliferation rate in Group I is increased by 60% in comparison with the proliferation rate without piezoelectric stimulation. From Fig. 3(b), the signals generated from pulling the leg of the SD rat were relatively small. Because the SD rat experiment is for the purpose of proving the concept, the pulling forces used in that testing were very gentle (~ 0.5 N). In the cell proliferation test, as shown in Fig. 1, the pressed nanofiber bundles were excited by the speaker underneath the

Flexcell culture plate, which generated much more forces than the ones used in the pulling leg experiment. As the data shown in Fig. 3(b), the signals generated from the excited speaker are much more than the ones from the pulling leg experiment in Fig. 4(b). We believe that the electrical stimulation generated by the poled piezoelectric scaffolds plays a critical role in enhancing the proliferation of L929 fibroblast cells. This experimental result revealed that cells can be stimulated on a piezoelectric scaffold by the surface charge from a mechanical vibration which can greatly enhance cell proliferation. In addition, the experiment demonstrates that piezoelectric scaffolds can be designed for specific tissue scaffolding purposes to provide the necessary electrical stimulation for wound healing applications.

In this paper, it was systematically investigated how electrospinning parameters could affect the piezoelectricity of the electrospun PVDF-TrFE nanofibers. Especially, it was found that piezoelectric coefficient would achieve the maximum value if the collecting distance (between the needle and rotating mandrel) was set to 10 cm. Previous study indicated that the piezoelectricity can be directly obtained from the as-spun PVDF nanofibers¹⁷. However in this paper, we found that one has to use a DC poling method to obtain a stable piezoelectricity in electrospun PVDF-TrFE nanofibers. Next, instead of using complicated Flexcell tension plus system (Flexcell, FX-4000T, USA), it was designed for the first time in this investigation that a simple speaker structure can be used to excite the piezoelectricity from the electrospun PVDF-TrFE nanofibers. Furthermore, it was found that the electrospun PVDF-TrFE nanofibers can improve the cell proliferation rate by 60% using piezoelectric stimulation.

4. Conclusion

In this paper, it was systematically investigated how electrospinning parameters could affect the piezoelectricity of the electrospun PVDF-TrFE nanofibers. Especially, it was found that piezoelectric coefficient can be affected by collecting distance (between the needle and rotating

mandrel) and solution concentration. An intermediate distance (10 cm) is the optimized electrospinning distance to generate the large piezoelectricity on the PVDF-TrFE nanofibers. After the poling process, the electrospun PVDF-TrFE nanofibers fabricated under these optimized electrospinning conditions showed a remnant polarization (P_r) and d_{31} of poled P(VDF-TrFE) NFSs of ~ 42.5 mC/m² and 16.17 pC/N, respectively. Under mechanical vibration, the poled P(VDF-TrFE) NFS can generate an electrical output of 0.75 V and 22.5 nA. After implanted under the skin of the rat's leg, the peak output voltage and output current of a polarized P(VDF-TrFE) NFS could reach ~ 6 mV and around ~ 6 nA. Further, the electrospun P(VDF-TrFE) nanofibrous scaffolds (NFSs) were used for cell alignments and proliferation experiment. The SEM images show that L929 cells align perfectly along the electrospinning direction of the nanofibers. Further, it was found that, once the fibroblast cells were stimulated under the surface charges from the poled electrospun P(VDF-TrFE) nanofiber scaffolds, the cell proliferation rate can enhance 1.6 fold as compared with the unpoled P(VDF-TrFE) scaffold. Due to good cytocompatibility, effective cell elongation, and a greatly enhanced cell proliferation rate, electrospun P(VDF-TrFE) nanofiber scaffolds show excellent potential for tissue engineering and bone regeneration applications.

Acknowledgments

This research was supported by the National Key R&D Project from the Ministry of Science and Technology in China under Grant nos. 2016YFA0202702, 2016YFA0202703, the National Natural Science Foundation of China under Grant nos. 51673027, 31571006, 81601629, Beijing Talents Fund (2015000021223ZK21) and "Thousands Talents" program for pioneer researcher and his innovation team.

Appendix A. Supplementary material

Supplementary data associated with this article can be found in the online version at <http://dx.doi.org/10.1016/j.nanoen.2017.11.023>.

References

- [1] H.S. Burr, C.I. Hovland, *Yale J. Biol. Med.* 9 (1937) 247–258.
- [2] E. Fukada, I. Yasuda, *J. Phys. Soc. Jpn.* 12 (1957) 1158–1162.
- [3] R.O. Becker, J.A. Spadro, *Bull. N.Y. Acad. Med.* 48 (1972) 627–641.
- [4] D. Assimakopoulos, *Am. Surg.* 34 (1968) 423–431.
- [5] J.C. Weaver, R.D. Astumian, *Science* 247 (1990) 459–462.
- [6] M. Zhao, B. Song, J. Pu, T. Wada, B. Reid, G. Tai, F. Wang, A. Guo, P. Walczysko, Y. Gu, T. Sasaki, A. Suzuki, J.V. Forrester, H.R. Bourne, P.N. Devreotes, C.D. McCaig, J.M. Penninger, *Nature* 442 (2006) 457–460.
- [7] J.T. Seil, T.J. Webster, *Int. J. Nanomed.* 3 (2008) 523–531.
- [8] Y. Qu, D. Ao, P. Wang, Y. Wang, X. Kong, Y. Man, *J. Bioact. Compat. Polym.* 29 (2014) 3–14.
- [9] C. Ribeiro, S. Moreira, V. Correia, V. Sencadas, J.G. Rocha, F.M. Gama, J.L. Gomez Ribelles, S. Lanceros-Mendez, *RSC Adv.* 2 (2012) 11504–11509.
- [10] C. Ribeiro, J. Parssinen, V. Sencadas, V. Correia, S. Miettinen, V.P. Hytonen, S. Lanceros-Mendez, *J. Biomed. Mater. Res. Part A* 103 (2015) 2172–2175.
- [11] Q.M. Zhang, C. Huang, F. Xia, J. Su, *Electroactive Polymer (EAP) Actuators as Artificial Muscles*, SPIE Press, Washington, 2004.
- [12] A.J. Lovinger, *Science* 220 (1983) 1115–1121.
- [13] A.J. Lovinger, G.T. Davis, T. Furukawa, M.G. Broadhurst, *Macromolecules* 15 (1982) 323–328.
- [14] P. Hitscherich, S. Wu, R. Gordan, L.H. Xie, T. Arinze, E.J. Lee, *Biotechnol. Bioeng.* 113 (2016) 1577–1585.
- [15] Y.S. Lee, G. Collins, T.L. Arinze, *Acta Biomater.* 7 (2011) 3877–3886.
- [16] N. Weber, Y.S. Lee, S. Shanmugasundaram, M. Jaffe, T.L. Arinze, *Acta Biomater.* 6 (2010) 3550.
- [17] H.F. Guo, Z.S. Li, S.W. Dong, W.J. Chen, L. Deng, Y.F. Wang, D.J. Ying, *Colloid Surf. B* 96 (2012) 29.
- [18] G.G. Genchi, L. Ceseracciu, A. Marino, M. Labardi, S. Marras, F. Pignatelli, L. Bruschini, V. Mattoli, G. Ciofani, *Adv. Healthc. Mater.* 5 (2016) 1808–1820.
- [19] X. Zhang, C. Zhang, Y. Lin, P. Hu, Y. Shen, K. Wang, S. Meng, Y. Chai, X. Dai, X. Liu, Y. Liu, X. Mo, C. Cao, S. Li, X. Deng, L. Chen, *ACS Nano* 10 (2016) 7279–7286.
- [20] D. Farrar, K. Ren, D. Cheng, S. Kim, W. Moon, W.L. Wilson, J.E. West, S.M. Yu, *Adv. Mater.* 23 (2011) 3954–3958.
- [21] G. Zhao, B. Huang, J. Zhang, A. Wang, K. Ren, Z. Wang, *Macromol. Mater. Eng.* 22 (2017) 222905.
- [22] K. Ren, W.L. Wilson, J.E. West, Q.M. Zhang, S.M. Yu, *Appl. Phys. A-Mater.* 107 (2012) 639–646.
- [23] Y. Wang, K. Ren, Q.M. Zhang, *Appl. Phys. Lett.* 91 (2007) 222905.
- [24] K. Ren, Y. Liu, H. Hofmann, Q.M. Zhang, J. Blottman, *Appl. Phys. Lett.* 91 (2007) 132910.
- [25] D. Dhakras, V. Borkar, S. Ogale, J. Jog, *Nanoscale* 4 (2012) 752.
- [26] Z. Xu, M. Baniyadi, S. Moreno, J. Cai, M. Naraghi, M. Minary-Jolandan, *Polymer* 106 (2016) 62–71.
- [27] L. Zhou, G. Zhu, R. Yang, et al., *Adv. Mater.* 22 (2010) 2534–2537.
- [28] Q. Zheng, B. Shi, F. Fan, et al., *Adv. Mater.* 26 (2014) 5851–5856.
- [29] Q. Zheng, Y. Zou, Y. Zhang, et al., *Sci. Adv.* 2 (2016) e1501478.
- [30] S.A. Sydlik, S. Jhunjhunwala, M.J. Webber, D.G. Anderson, R. Langer, *ACS Nano* 9 (2015) 3866–3874.



Aochen Wang is a Ph.D. candidate in Tianjin University and she is also an exchange student in Beijing Institute of Nanoenergy and Nanosystems. Her current research interests focus on piezoelectric materials and MEMS based nano sensors



Zhuo Liu received the B.S. degree and the M.S. degree from Gannan medical University and Beihang University, China, in 2014 and 2017, respectively. He is currently working toward the Ph.D. degree at the Beihang University, Beijing, China. His research work is focused on nanogenerator, biosensors and biomechanics.



Ming Hu, she is professor at School of Microelectronics, Tianjin University. She is also a senior member of the Chinese Institute of Electronics, China Vacuum Society and Chinese Society of Micro-Nano Technology. Her research work is focused on sensitive materials and micro-nano sensors.



Yu-Bo Fan is the Dean of School of Biological Science and Medical Engineering, Director of Key Laboratory for Biomechanics and Mechanobiology of Ministry of Education of Beihang University, Director of National Research Centre for Rehabilitation Technical Aids of China. He is the AIMBE Fellow, the President of Chinese Biomedical Engineering Society, Chair elect of World Association for Chinese Biomedical Engineers (WACBE), Vice president of China Strategic Alliance of Medical Devices Innovation, and Council Member of World Congress of Biomechanics. Prof. Fan specializes in biomechanics, mecha-nobiology, and biomaterials.



Zhou Li, Ph.D., professor. He received his Ph.D. from Peking University in Department of Biomedical Engineering in 2010, and Medical Degree from Wuhan University in Medical School, 2004. He joined School of Biological Science and Medical Engineering of Beihang University in 2010 as an associate Professor. Currently, he is a Professor in Beijing Institute of Nanoenergy and Nanosystems, CAS. His research interests include nanogenerators, in vivo energy harvester and self-powered medical devices, biosensors.



Kailiang Ren, Ph.D., professor. He obtained his M.S. and Ph.D. degree from the Pennsylvania State University in 2005 and 2007, respectively. He was a postdoctoral fellow at the Pennsylvania State University from 2009 to 2010 and Johns Hopkins University from 2011 to 2014. Currently, he is a professor at Beijing Institute of Nanoenergy and Nanosystems. His primary research interests focus on device applications of novel electronic materials, especially soft electronic materials and ferroelectric-based materials, which include piezoelectric nanofiber based nanogenerators, energy devices for electrical energy storage and conversion, and MEMS sensors. He has authored and co-authored over 30 *publications*, one US patent and 2 patents

pending.